Electrochemistry of Triazenes, 3[1]

One-Electron Oxidation of Aryltriazenes to Radical Cations

Lothar Dunsch[a], Bernhard Gollas[b], Andreas Neudeck[a], Andreas Petr[a], Bernd Speiser*[b], and Hartmut Stahl[b]

Abteilung Elektrochemie und leitende Polymere, Institut für Festkörper- und Werkstofforschung[a], Helmholtzstraße 20, D-01069 Dresden, Germany

Institut für Organische Chemie[b], Universität Tübingen, Auf der Morgenstelle 18, D-72076 Tübingen, Germany
e-mail: bs@echem3.orgchemie.chemie.uni-tuebingen.de

Received May 6, 1994

Key Words: Triazenes, aryl / Radical cations / Cyclic voltammetry / ESR spectroscopy / UV-Vis spectroelectrochemistry

3,3-Dimethyl-1-(4-R-phenyl)- [R = $(CH_3)_2N$, C_2H_5O, CH_3O, CH_3; **3**] and 3-Methyl-1-(4-R^1-phenyl)-3-(4-R^2-phenyl)triazenes [R^1 = $(CH_3)_2N$, CH_3O, NO_2, R^2 = CH_3O, H, **4**] are oxidized electrochemically and chemically to their one-electron oxidation products. Cyclic voltammograms of the triazenes are discussed, and ESR as well as UV/Vis spectra of the radical cations are presented. The stability of the triazene radical cations generated depends on the substituents on the aryl rings. 4-R-Benzenediazonium ions are identified as one of the decay products of the radical cations by means of cyclic voltammetry and UV/Vis spectroelectrochemistry.

Triazenes **1** are not only used in synthesis, e.g. for alkylations[2] or generation of intermediate pyridynes[3], but are also applied as herbicides[4], fungicides[5,6], and insecticides[7]. Recently, a specific triazene, 5-(3,3-dimethyl-1-triazenyl)imidazole-4-carboxamide, DTIC (**2**), has been introduced as a chemotherapeutic agent against malignant melanoma[8,9] and "second-generation" antitumor *N*-aryl-*N'*,*N'*-dialkyltriazenes[10] are being developed. On the other hand, triazenes are regarded as carcinogenic compounds[11]. The biochemical effects of **1** have been related to oxidative intermediate species[8,11,12]. The *primary* product of a one-electron oxidation of a triazene is expected to be a triazene radical cation according to reaction (1).

$$\mathbf{1} \rightleftharpoons \mathbf{1}^{\bullet+} + e^- \qquad (1)$$

This electron transfer reaction might be performed either by chemical or electrochemical means. Although some reports have appeared regarding the electrochemical *reduction* (see e.g. ref.[13]), only few references in the literature of triazenes discuss the anodic *oxidation* of these compounds[14–16].

Evidence for the occurrence of a triazene radical cation has recently been provided[17] from cyclic voltammetric and ESR spectroscopic investigations of 1-[4-(dimethylamino)-phenyl]-3,3-dimethyltriazene (**3a**) in acetonitrile. Radical cation $\mathbf{3a}^{\bullet+}$ decays only slowly, and as a product of the reaction Wursters Blue radical cation is detected. The oxidation of 1,3-diaryltriazenes **4a–c**, on the other hand, leads to the formation of a dimethoxy-substituted phenazine radical cation[18].

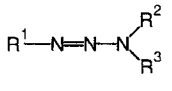

1

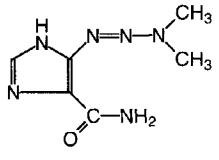

2

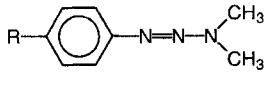

3	R
a	$N(CH_3)_2$
b	OC_2H_5
c	OCH_3
d	CH_3

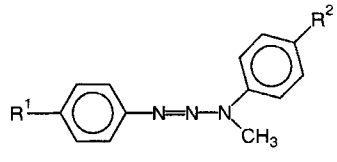

4	R^1	R^2
a	$N(CH_3)_2$	OCH_3
b	NO_2	OCH_3
c	OCH_3	OCH_3
d	OCH_3	H

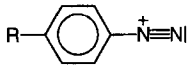

5	R
a	$N(CH_3)_2$
b	OC_2H_5
c	OCH_3
d	NO_2

In the present paper, we report on the electrochemical and chemical one-electron oxidation of several triazenes **3** and **4** which form persistent or only slowly reacting primary paramagnetic oxidation products. Thus, the first examples of triazene radical cation ESR and UV/Vis spectra are presented, the existence of such species is further substantiated and one of their decay products identified.

  0009–2940/94/1212–2423 $ 10.00+.25/0

Results and Discussion

Cyclic Voltammetry of 3, ESR Spectroscopy of $3^{\bullet+}$, and UV/Vis Spectroelectrochemistry of $3/3^{\bullet+}$

Cyclic voltammetry of **3a** (E^0 = +0.091 ± 0.001 V) has already shown that $\mathbf{3a}^{\bullet+}$ exhibits sufficient stability for detection (rate constant of decay $k \approx 0.01\ s^{-1}$)[17]. With a conventional ESR spectroscopic experiment, however, even at −40°C only spectra are obtained which are possibly superimposed by the Wursters Blue spectrum[17].

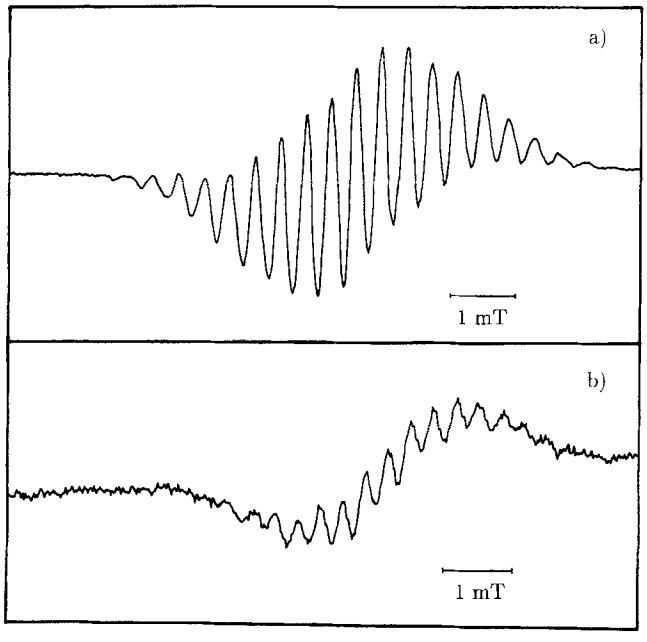

Figure 1. ESR spectra of 1-aryl-3,3-dimethyltriazene radical cations; a) $\mathbf{3a}^{\bullet+}$, b) $\mathbf{3b}^{\bullet+}$

Experiments performed with a rapid-scan ESR spectrometer and in situ anodic oxidation result in the spectrum shown in Figure 1a. Lines of the Wursters Blue spectrum are not found. After prolonged experimentation, the spectrum shown disappears and the Wursters Blue spectrum appears. Only if strictly anaerobic and anhydrous conditions are applied, Wursters Blue cannot be found even after longer times.

The spectrum of the primary oxidation product is composed of rather broad lines (distance of maxima ≈ 0.41 mT). Some of the nitrogen nuclei and the CH_3 protons seem to have similar coupling constants resulting in an unresolved spectrum. From the charge transferred during the in situ electrolysis and the spin concentration determined after generation of the radical cation, the number of electrons per oxidized molecule is found to be in the range n = 0.9 − 1.2. Thus, the species investigated is indeed a one-electron oxidation product, and the spectrum is attributed to $\mathbf{3a}^{\bullet+}$.

Figure 2 shows selected UV/Vis-spectroelectrochemical results recorded during cyclic voltammetry of **3a** at a honeycomb microstructured Au-LIGA electrode in a thin-layer spectroelectrochemical cell[19] (v = 0.442 Vs^{-1}). Spectrum 1 is found at the switching potential E_λ = +0.25 V, i.e. when most of **3a** has been converted into $\mathbf{3a}^{\bullet+}$ within the small electrolyte volume. The spectra are referred to that of **3a** (recorded at the starting potential E_{start} = −0.15 V of the voltammetric scan). Thus, disappearance of the triazene is indicated by negative absorbance values in the short wavelength part of the curve, where only the starting compound absorbs. The radical cation produced during the oxidation shows two absorption bands at λ_{max} = 450 nm (lg ε = 4.00) and 705 (3.56).

After the voltammetric cycle has been completed, the spectrum of the triazene is essentially recovered in its full intensity. Thus, the difference spectrum (spectrum 2 in Figure 2) shows no signal. We conclude that $\mathbf{3a}^{\bullet+}$ is stable on the time scale of this experiment and can be reduced to the reactant **3a** during the reverse scan of the voltammogram, in full accordance with the cyclic voltammetric results[17].

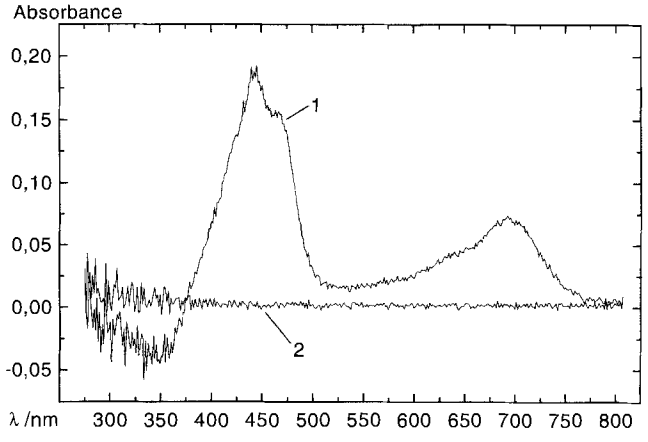

Figure 2. UV/Vis spectra recorded during cyclic voltammetry of **3a**, both curves referred to the spectrum of the triazene taken at the start of the potential cycle; 1: spectrum at the switching potential E_λ = +0.25 V, 2: spectrum recorded after a complete voltammetric cycle

Cyclic voltammograms of **3b** (Figure 3; oxidation peak potential E_p^I = +0.651 ± 0.002 V at v = 0.1 Vs^{-1}) show that this triazene is oxidized at more positive potentials than **3a**. At v = 0.2 Vs^{-1} an oxidation peak current function $i_p^I/(c\sqrt{v})$ approximately equal to that of **3a** is found, suggesting that again the one-electron oxidation product is formed. The decrease of the reduction peak II with decreasing scan rate indicates a faster decay reaction of $\mathbf{3b}^{\bullet+}$ as compared to $\mathbf{3a}^{\bullet+}$. The peak current function of the oxidation peak increases by more than 30% when v is decreased to 0.01 Vs^{-1}. Thus, in the latter experiments on a slower time scale, the product of the decay reaction is further oxidized at the electrode (ECE reaction). Reduction peak III in the negative potential region corresponds to the electrode reaction of the 4-ethoxybenzenediazonium ion **5b**, as is shown by a comparison with the cyclic voltammogram of an authentic sample of **5b** tetrafluoroborate.

By application of rapid-scan ESR spectroscopy and in situ anodic oxidation of **3b** it has been possible to record an ESR spectrum which we assign to $\mathbf{3b}^{\bullet+}$ (Figure 1b) and which shows a hyperfine splitting pattern with maxima separated by approximately 0.35 mT. The low resolution does

not allow us to assign coupling constants to N or H nuclei in the paramagnetic species.

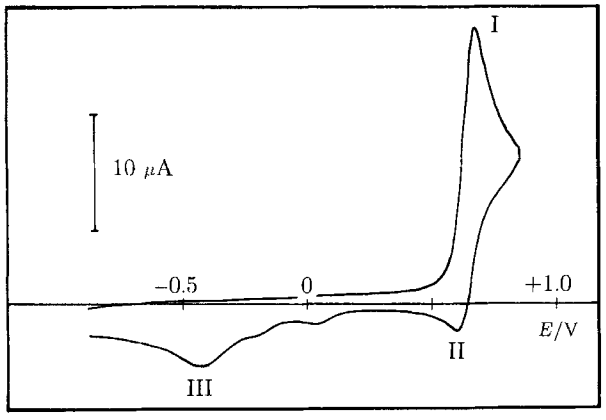

Figure 3. Cyclic voltammogram of 1-(4-ethoxyphenyl)-3,3-dimethyltriazene (**3b**), $v = 0.1$ Vs^{-1}, $c = 0.83$ mM

UV/Vis-spectroelectrochemical experiments are performed with **3b** at the Au-LIGA electrode. The time dependence of the spectra is shown in Figure 4. During 4.45 s a potential range +0.1 V → +1.15 V → +0.233 V is scanned with $v = 0.442$ Vs^{-1}. Thus, E increases during the first 2.38 s and then decreases again. At $t = 0$ s, two absorption bands A_1 and A_2 with $\lambda_{max} = 292$ nm (lg $\varepsilon = 4.10$) and 326 (4.07) are found, which we attribute to the neutral triazene. Upon an increase of the potential a current begins to flow. Simultaneously, the two signals decrease and new ones appear: a sharp absorption band at 440 nm (B_1, lg $\varepsilon = 4.73$) and a flat maximum at wavelengths above 600 nm (B_2, lg $\varepsilon = 3.97$). Their intensity passes through a maximum during the forward scan of the cyclic voltammogram. A further band C_1 at 317 nm (lg $\varepsilon = 4.19$) and a shoulder C_2 (lg $\varepsilon = 3.45$) extending to approximately 400 nm start to appear with some time delay, when B_1 and B_2 have their maximum absorbance. Band C_1 overlaps with bands A_1 and A_2 of the starting compound.

The scan rate and the switching potential are varied in these experiments. If the scan is reversed in the ascent to voltammetric peak I at relatively fast scan rates ($v \geq 1.0$ Vs^{-1}), bands A_1/A_2 are reformed in the second part of the voltammetric cycle. The primary oxidation product with bands B_1 and B_2 is stable on this time scale. If, however, the switching potential is more positive or the scan rate is slower, complete conversion of the product exhibiting bands B_1/B_2 to the species with C_1/C_2 occurs, and no change of the spectra during the reverse scan is observed. Thus, after the primary oxidation of the triazene a follow-up reaction forms a secondary product absorbing at C_1/C_2.

At slow scan rates ($v = 0.05$ Vs^{-1}), the intensity of band C_1 also goes through a maximum and then slowly decreases. The secondary product obviously undergoes a further transformation. For scan rates $v > 0.3$ Vs^{-1}, however, this decay can be neglected, since no decrease of C_1 is observed on this faster time scale. For spectra at the latter scan rates, separation of the signals due to **3b** and the final product (bands C_1/C_2) is possible. Furthermore, with the spectra of

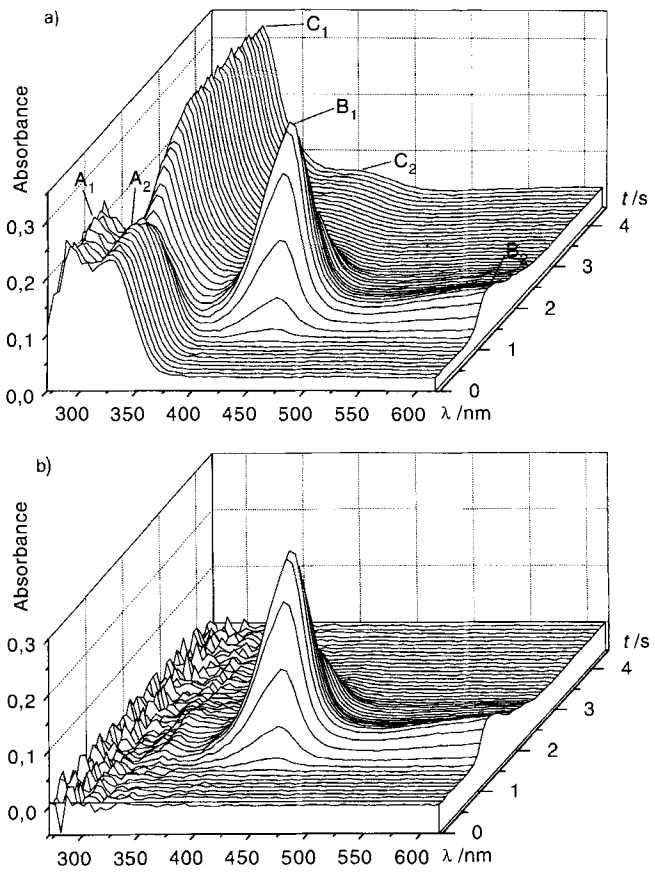

Figure 4. UV/Vis-spectroelectrochemical results for the electrode reaction of **3b** in acetonitrile/0.1 M NBu_4PF_6 at an Au-LIGA electrode; (a) time dependence of the spectra during a potential cycle with $v = 0.442$ Vs^{-1} and $E_{start} = +0.1$ V ($t = 0$ s), $E_\lambda = +1.15$ V ($t = 2.38$ s), as well as an end potential of +0.233 V ($t = 4.45$ s), $c = 1$ mM; (b) separated spectra of the radical cation **3b**$^{\bullet+}$

these species the spectrum of the primary oxidation product (bands B_1/B_2) can be calculated (Figure 4b).

In accordance with the cyclic voltammetric results, the primary oxidation product exhibiting bands B_1/B_2 is assumed to be the radical cation **3b**$^{\bullet+}$, while signals C_1/C_2 are attributed to the 4-ethoxybenzenediazonium ion **5b** (an authentic sample of **5b** tetrafluoroborate in acetonitrile shows $\lambda_{max} = 315$ nm).

Thus, the triazene radical cation **3b**$^{\bullet+}$ is formed by electrochemical oxidation of **3b** in acetonitrile at potentials of about +0.65 V (first E step in Scheme 1)[*] and decays to form the corresponding diazonium ion (C step in Scheme 1). Whether **5b** is produced directly by a cleavage of the N–N bond in **3b**$^{\bullet+}$ to give **5b** and a dimethylaminyl radical $(CH_3)_2N^\bullet$ or, alternatively, by intermediate formation of the corresponding diazenyl radical[20] (and its further oxidation) and $(CH_3)_2N^+$, cannot be decided on the basis of these results. Further oxidation (second E step in Scheme 1) of the neutral radical species formed would lead to two

[*] Only one of several possible mesomeric structures of the radical cation is shown. This formulation does not imply localization of the unpaired electron or the positive charge. Since the resolution of the spectra does not allow a detailed analysis of the spin densities, we cannot further specify the spin density and charge distribution.

cations, **5b** and $(CH_3)_2N^+$, in an ECE reaction sequence. Further side reactions (e.g. dimerization of the dimethylaminyl radical, cleavage of N_2 from the diazenyl radical, and hydrogen abstraction by the resulting phenyl radical) are possible, but no products of these pathways can be detected on the time scale of these experiments.

Scheme 1

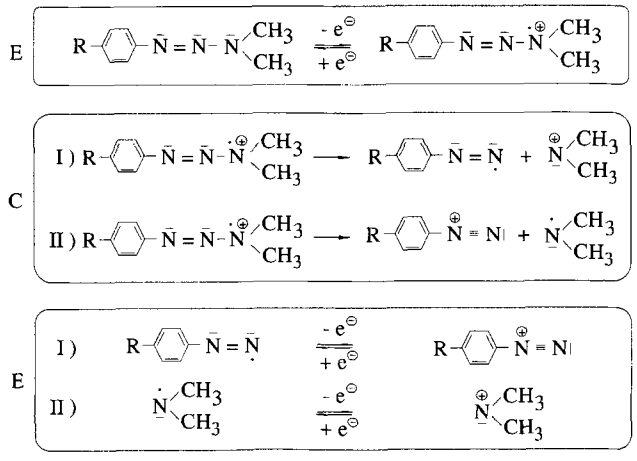

The cyclic voltammograms of **3c** and **3d** closely resemble that of **3b**. The peak potentials are shifted to higher potentials, however [E_p^I(**3c**) ≈ +0.67 and E_p^I(**3d**) ≈ +0.80 V at v = 0.2 Vs^{-1}]. The decay reactions of the corresponding radical cations are of a rate comparable to that of **3b**$^{\bullet+}$ in the case of **3c**$^{\bullet+}$, but faster in the case of **3d**$^{\bullet+}$.

Unresolved ESR spectra of **3c**$^{\bullet+}$ and **3d**$^{\bullet+}$ are detected during in situ electrochemical oxidation of **3c** and **3d**, respectively. No hyperfine splitting can be observed. The peak-to-peak difference in the spectra is about 2 mT in both cases.

The UV/Vis-spectroelectrochemical behavior of **3c** during a potential cycle is similar to that of **3b**. Again bands A_1/A_2 (λ_{max} = 292 and 320 nm; lg ε = 3.80 for both signals), B_1/B_2 (λ_{max} = 440 and 620 nm; lg ε = 4.42 and 3.70, respectively), and C_1 (λ_{max} = 310 nm, lg ε = 3.98) with a broad shoulder extending to approximately 440 nm (C_2, lg ε = 2.85) are observed and assigned to **3c**, **3c**$^{\bullet+}$, and **5c**, accordingly.

The g factors of the triazene radical cations **3a**$^{\bullet+}$–**d**$^{\bullet+}$ are given in Table 1. Their values are close to those found for mono-[21,22], di-[21,23], and triarylamine radical cations[21,23] as well as Wursters Blue (g = 2.0028 in the crystalline state)[24].

Table 1. The g factors of the investigated triazene radical cations

Compound	g	Compound	g
3a$^{\bullet+}$	2.0036[a]	**4a**$^{\bullet+}$	2.0028[b]
3b$^{\bullet+}$	2.0040[a]	**4b**$^{\bullet+}$	2.0031[b]
3c$^{\bullet+}$	2.0036[a]		
3d$^{\bullet+}$	2.0028[a]		

[a] Determined relative to DPPH. – [b] Determined relative to 4-*tert*-butoxy-2,6-di-*tert*-butylphenoxyl radical[34].

Cyclic Voltammetry of 4 and ESR Spectra of 4$^{\bullet+}$

Cyclic voltammograms of **4a–c** are presented in Figure 5. The dimethylamino-substituted triazene **4a** (Figure 5a) is oxidized in two reversible one-electron steps (peaks I, III) similar to **3a**[17] to form **4a**$^{\bullet+}$ and subsequently **4a**$^{2+}$. The oxidation products are reduced in peaks II and IV. Only slow follow-up reactions are coupled to the electron transfers. The diazonium ion **5a** produced in a small quantity is reduced at $E \approx -0.7$ V (peak V). A different pattern of peaks is found for the nitrotriazene **4b** (Figures 5b and c). The primary oxidation product generated in peak I is stable on the time scale of the voltammetric experiments, if the voltammogram is extended only to E_λ = +1.0 V. It is reduced in peak II (Figure 5b). The oxidation product generated in a second oxidation peak III, however, is unstable, and no corresponding reduction peak is found (Figure 5c). If the scan is extended to E_λ = +1.5 V, peak II decreases as compared to voltammograms with E_λ = +1.0 V. Now a smaller radical cation concentration remains near the electrode due to its further oxidation in peak III and the follow-up reaction of the two-electron oxidation product. The reduction of the diazonium ion is observed in peak V, which appears only after peak III has been reached before. Thus, **5b** is only produced as a product of the second electron transfer but not from **4b**$^{\bullet+}$ on the time scale of these voltammograms.

In the case of the methoxy-substituted compound **4c** (Figure 5d) even the primary oxidation product formed in peak I is not stable enough to be detected upon reversal of the potential scan. Peak III for the second oxidation process is only small, indicating that indeed the one-electron product undergoes a follow-up decay reaction and is no longer available for further oxidation. Peak V again results from the formation of the diazonium ion. A comparison of the experimental voltammograms with computer simulations proves the occurrence of an ECE reaction mechanism in peak I as in the case of **3b**. Further follow-up reactions are, however, coupled to the ECE sequence, which influence the cyclic voltammograms at slow scan rates.

In order to record ESR spectra of **4**$^{\bullet+}$, the one-electron products of the 1,3-diaryltriazenes **4a** and **4b** are generated by both chemical *and* electrochemical means. In the case of **4a**$^{\bullet+}$ electrochemical generation results in low signal intensities. Chemical oxidation yields much better spectra (Figure 6a). ESR spectra of **4b**$^{\bullet+}$ (Figure 6b) are independent of the technique by which the species are produced, although the spectra of the chemically oxidized species usually show less noise.

As expected from the cyclic voltammetric results, the radical cations **4a**$^{\bullet+}$ and **4b**$^{\bullet+}$ are relatively persistent and decay only slowly. If spectra are recorded repeatedly over longer periods of time, however, the intensity of the radical cation spectral lines decreases while those of the 2,7-dimethoxy-5,10-dimethyl-5,10-dihydrophenazine radical cation[18,25] appear. In the case of **4c**, the latter paramagnetic species is formed much more rapidly, and the primary triazene radical cation **4c**$^{\bullet+}$ cannot be detected. This result is in

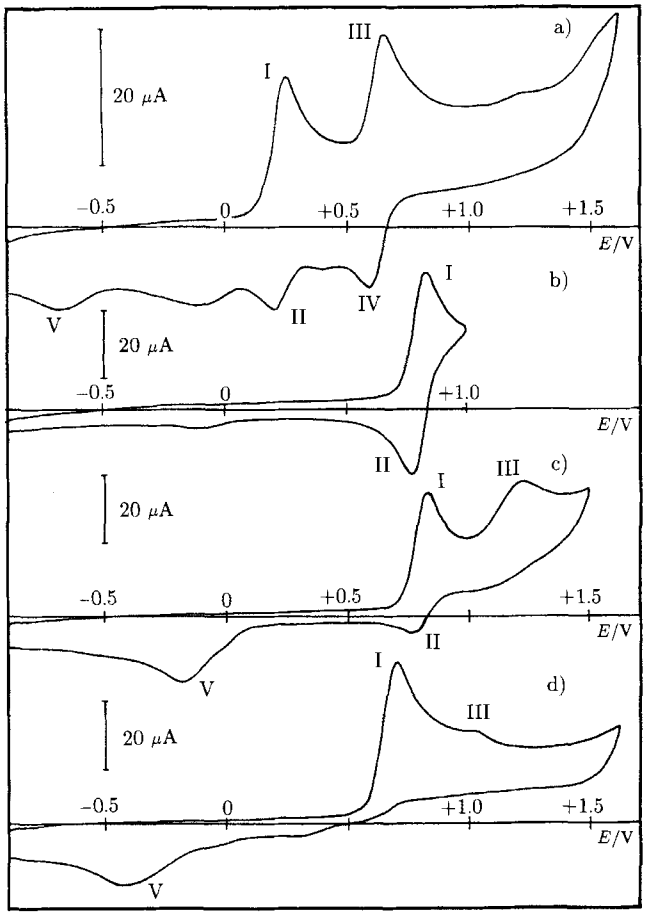

Figure 5. Cyclic voltammograms of 1,3-diaryl-3-methyltriazenes **4a–c**, a) **4a**, $v = 0.1$ Vs^{-1}, $c = 0.84$ mM, b) and c) **4b**, $v = 0.2$ Vs^{-1}, $c = 0.92$ mM, d) **4c**, $v = 0.1$ Vs^{-1}, $c = 1.19$ mM

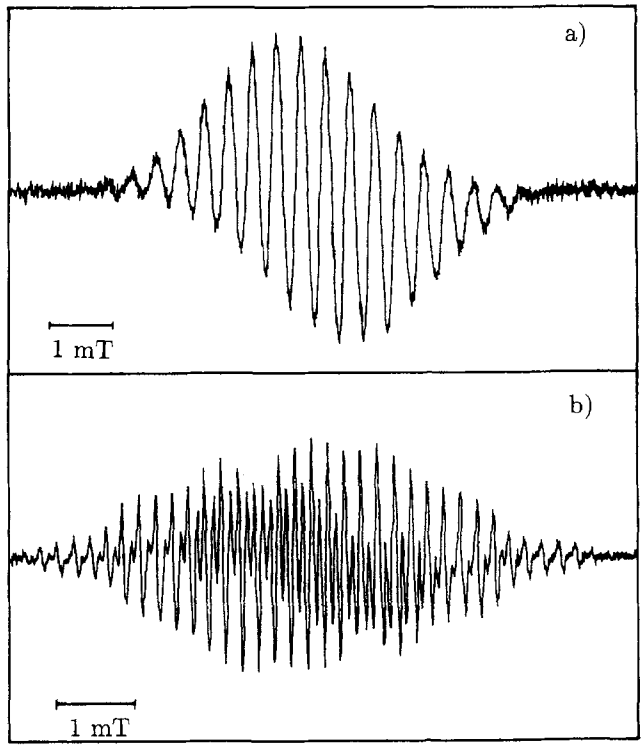

Figure 6. ESR spectra of 1,3-diaryl-3-methyltriazene radical cations; a) **4a**$^{\bullet+}$, $T = -40$°C, b) **4b**$^{\bullet+}$, $T = 20$°C

accordance with the faster decay of the oxidation product of **4c**, also shown by the cyclic voltammograms. A corresponding triazene radical cation cannot be detected during chemical oxidation of **4d**.

As in the case of **3a**$^{\bullet+}$ and **3b**$^{\bullet+}$, the ESR spectrum of **4a**$^{\bullet+}$ is only partly resolved. The signals show a splitting of 0.38 mT. The ESR spectrum of **4b**$^{\bullet+}$ clearly shows more and sharper lines than those of the **3**$^{\bullet+}$ discussed above and **4a**$^{\bullet+}$. However, a determination of the coupling constants is still not possible.

The *g* factors of the triazene radical cations **4a**$^{\bullet+}$ and **4b**$^{\bullet+}$ are given in Table 1.

It is surprising that the two radical cations **4a**$^{\bullet+}$ and **4b**$^{\bullet+}$ possess similar persistency although in **4a**$^{\bullet+}$ the strongly electron-donating dimethylamino group should contribute to the delocalization of the positive charge and the unpaired electron, while the strongly electron-withdrawing NO_2 group should rather destabilize **4b**$^{\bullet+}$.

We attribute this behavior to a push-pull stabilization (capto-dative effect[26]) of the radical cation in the nitro-substituted compound. Valence bond formulations show that several additional mesomeric structures are possible for a 1,3-diaryltriazene which bears a donor *and* an acceptor group in the two *para* positions of the aryl rings, respectively, as compared to a compound with two donor substituents.

Conclusion

The results presented here confirm that the one-electron oxidation products of triazenes **3** and **4** exist and that they are persistent enough to be detected by electrochemical and spectroscopic means. Several radical cations of the types **3**$^{\bullet+}$ and **4**$^{\bullet+}$ have been characterized by ESR and UV/Vis spectroscopy upon electrochemical or chemical oxidation. The formation of a one-electron oxidation product was proven by quantitative determination of the radicals formed in relation to the charge transferred. Due to the large number of coupling nuclei, however, a detailed analysis of the ESR spectra and an analysis of structural details of the triazene radical cations was not possible. On the other hand, even state-of-the-art calculations of spin densities seem not to be reliable enough for an estimation of coupling constants without comparison to experimental results.

The stability of the triazene radical cations decreases with decreasing electron donating effect of the *para* substituent R in the 1-aryl moiety with the exception of **4b**$^{\bullet+}$, where push-pull stabilization appears to contribute to the persistency of the radical cation species. Both cyclic voltammetry and UV/Vis spectroelectrochemistry show the formation of 4-R-benzenediazonium ions **5** as a result of the decay of the triazene radical cations. Thus, cleavage between N^2 and N^3 of the triazene nitrogen chain is an important reaction of the triazene radical cations.

The authors thank the *Deutsche Forschungsgemeinschaft* and the *Fonds der Chemischen Industrie* for financial support. Discussions

with Dr. *J. Salbeck* regarding the UV/Vis spectroelectrochemical experiments are greatfully acknowledged. We thank Professor *J. Strähle* of the Institut für Anorganische Chemie der Universität Tübingen for the possibility of using a UV/Vis spectrometer. The fast-scan UV/Vis spectroelectrochemical experiments were supported by Professor *R. N. Schindler* and Dr. *J. Posdorfer* (Universität Kiel) as well as Dr. *P. Ullmann* (Carl Zeiss GmbH, Jena).

Experimental

NMR (250 MHz): Bruker AC 250, tetramethylsilane as internal standard. – MS (EI): Finnigan TSQ 70. – ESR: Bruker ESP 300, Bruker ESP 300 E, or an ERS 221 from the Centre of Scientific Instruments, Berlin. Experimental details of the in situ ESR experiments with potential-controlled anodic oxidation of the compounds **3** are described elsewhere[27]. ESR spectra of the $\mathbf{4}^{\bullet+}$ were recorded in CH_3CN/0.1 M NBu_4PF_6 after purging with N_2. The radicals were either generated electrochemically in a flat cell under control of the cell voltage or chemically by the addition of I_2 ($\mathbf{4a}^{\bullet+}$) or $I_2/AgClO_4$ ($\mathbf{4b}^{\bullet+}$). – UV: Shimadzu UV-2100 (for conventional spectra), Tracor Northern TN 6500 or Zeiss-MCS 320 (for spectroelectrochemical experiments). In the UV/Vis-spectroelectrochemical experiments, an Au-LIGA electrode of 2.10 mm diameter (honeycombed microstructure with hexagon-shaped tubes, 110 μm thick; distance of opposite hexagon edges: 25 μm, distance of two hexagons: 15 μm) was used. The thin-layer UV/Vis-spectroelectrochemical cell is described in detail elsewhere[19]. With the Tracor Northern spectrometer, during a cyclic potential scan (range: +0.1 V ≤ E ≤ +1.15 V) 60 spectra were recorded (spectroelectrochemistry of **3a**). Each spectrum was measured within 5 ms. In the case of the Zeiss-MCS 320, the spectroscopic and electrochemical parts of the experiment were synchronized by a trigger signal at t = 0 s and 50 spectra (duration: 22 ms each) were taken at 90.8-ms intervals. Thus, the last spectrum was recorded at +0.233 V on the reverse scan of the cyclic voltammogram. A silver wire covered with AgCl was used as an internal reference electrode during the experiments. The separation of the spectra due to **3**, $\mathbf{3}^{\bullet+}$, and **5** is described in the following for the example of the 4-ethoxy species (Figure 4). Data in the range 270 nm ≤ λ ≤ 355 nm were used, where absorption of $\mathbf{3b}^{\bullet+}$ does not interfere with the absorptions of either the triazene or the diazonium ion. Also, the scan rate was selected such that no decay of **5b** had to be taken into account (v = 0.442 Vs^{-1}). The first spectrum recorded at E = +0.1 V (t = 0 s, beginning of the potential scan) corresponds to the spectrum of **3b** (c = 1 mM), while the last one is regarded as a spectrum of **5b** in 1 mM concentration. The mixed spectra in the range of wavelengths given above were then separated by linear regression. Subtraction of the resulting spectra of **3b** and **5b** from the total spectra leaves the signal of the triazene radical cation $\mathbf{3b}^{\bullet+}$. – Cyclic voltammetry: Bruker Polarograph E 350/Wenking Voltage Scan Generator MVS 87/Houston Instruments Omnigraphic 2000 recorder, working electrode: Pt disk (Metrohm electrode tip, electroactive area $A \approx 0.07$ cm^2), counter electrode: Pt wire (1 mm diameter), reference electrode: Ag/Ag^+ (0.01 M) in CH_3CN connected to the cell via a Haber-Luggin capillary, solvent: CH_3CN [dried with $CaCl_2$, distilled over P_2O_5, NaH, and again P_2O_5, passed over a column of alumina (neutral, Brockmann activity I)], supporting electrolyte: NBu_4PF_6, 0.1 M. All potentials given in this paper are referred to an external ferrocene/ferricinium standard.

Synthesis of Triazenes: Triazenes **3** and **4** were prepared by coupling of the corresponding 4-R-benzenediazonium salts with dimethylamine (**3**), *N*-methylamine (**4d**), or *N*-methyl-*p*-anisidine (**4a–c**) according to general procedures[28–32]. Synthesis and spectroscopic properties of compounds **3**[28,29] and **4c**[30,32] had been reported before. Spectra of the triazenes were in accordance with the literature data.

1-[4-(Dimethylamino)phenyl]-3-(4-methoxyphenyl)-3-methyltriazene (**4a**): 0.48 g (3.5 mmol) of *N,N*-dimethyl-*p*-phenylenediamine was diazotized in HCl[33]. 0.48 g (3.5 mmol) of *N*-methyl-*p*-anisidine was dissolved in 3 ml of MeOH and 1 ml of a 3 M aqueous solution of NaAc. With stirring and cooling (T < 5°C) the anisidine solution was added to the solution of the diazonium salt. The reaction mixture was adjusted to a pH of 9 by addition of 4 M NaOH and the NaAc solution. After stirring for 1 h, addition of an excess of water, and additional stirring, a brown precipitate was filtered off, washed with water, and dried overnight. Recrystallization from petroleum ether (60/90) produced some black tar, from which the hot solution was separated. After cooling, a yellow solid formed which was collected and recrystallized from MeOH. This procedure yielded 0.08 g of **4a** (8%). Yellow solid, m.p. (MeOH) 134°C. – ^{1}H NMR ([D$_6$]acetone): δ = 2.96 [s, 6H, $N(CH_3)_2$], 3.56 (s, 3H, NCH_3), 3.80 (s, 3H, OCH_3), 6.78 (d, 2H, aromat.), 6.98 (d, 2H, aromat.), 7.43 (d, 2H, aromat.), 7.47 (d, 2H, aromat). – ^{13}C NMR ([D$_6$]acetone): 32.6 (q, NCH_3), 40.6 [q, $N(CH_3)_2$], 55.6 (q, OCH_3), 113.3 (d, aromat.), 115.1 (d, aromat.), 118.9 (d, aromat.), 122.6 (d, aromat.), 139.6 (d, aromat.; only in [D$_6$]DMSO), 140.9 (d, aromat.; only in [D$_6$]DMSO), 150.0 (d, aromat.; only in [D$_6$]DMSO), 156.2 (d, aromat.; only in [D$_6$]DMSO). – MS (70 eV), *m/z* (%): 284.1 (3) [M$^+$], 256.0 (2), 148.0 (32), 136.1 (28), 120.1 (100). – $C_{16}H_{20}N_4O$ (284.4): calcd. C 67.58, H 7.09, N 19.70; found C 67.45, H 7.08, N 18.13. – The color of the triazene turns into brown upon exposure to air within a few days.

3-(4-Methoxyphenyl)-3-methyl-1-(4-nitrophenyl)triazene (**4b**): 0.48 g (3.5 mmol) of 4-nitroaniline was diazotized in HCl[33]. 0.48 g (3.5 mmol) of *N*-methyl-*p*-anisidine was dissolved in MeOH. A 3 M aqueous solution of NaAc was added up to a volume of 3–3.5 ml. With stirring and cooling (T < 5°C) the solution of the diazonium salt was added to the anisidine solution in this case. Further workup was carried out as in the case of the synthesis of **4a**. Recrystallization from acetonitrile and then from methanol afforded 0.49 g of **4b** (49%). Orange needles, m.p. (MeOH) 127°C. – ^{1}H NMR ([D$_6$]acetone): δ = 3.73 (s, 3H, NCH_3), 3.83 (s, 3H, OCH_3), 7.04 (d, 2H, aromat.), 7.54 (d, 2H, aromat.), 7.72 (d, 2H, aromat.), 8.27 (d, 2H, aromat.). – ^{13}C NMR ([D$_6$]acetone): 35.5 (q, NCH_3), 55.8 (q, OCH_3), 115.2 (d, aromat.), 120.7 (d, aromat.), 122.1 (d, aromat.), 125.5 (d, aromat.), 139.0 (d, aromat.), 146.1 (d, aromat.), 156.5 (d, aromat.), 158.4 (d, aromat.). – MS (70 eV), *m/z* (%): 286.1 (3) [M$^+$], 258.1 (1), 150.0 (2), 136.0 (100), 121.9 (13). – $C_{14}H_{20}N_4O_3$ (286.3): calcd. C 58.74, H 4.93, N 19.57; found C 58.55, H 5.20, N 19.82.

[1] For part 2, see ref. [18].
[2] K. Vaughan, M. F. G. Stevens, *Chem. Soc. Rev.* **1978**, *7*, 377–397.
[3] S. P. Modi, S. Archer, *J. Org. Chem.* **1989**, *54*, 5189–5190.
[4] M. Mazza, G. Pagani, G. Calderara, L. Vicarini, *Farmaco, Ed. Sci.* **1974**, *29*, 58–72.
[5] F. H. Adams, D. P. Wright Jr., U. S. Patent 3,162,571, Dec. **1964**; *Chem. Abstr.* **1964**, *62*, 14568f.
[6] J. Takahashi, S. Nakamura, Jap. Patent 62,273,941 [87,273,941], May **1986**; *Chem. Abstr.* **1988**, *109*, 68839e.
[7] M. Mazza, L. Montanari, F. Pavanetto, T. Modena, *Farmaco, Ed. Sci.* **1982**, *37*, 548–554.
[8] M. Julliard, G. Vernin, *Ind. Eng. Chem. Prod. Res. Dev.* **1981**, *20*, 287–296.
[9] T. Giraldi, T. A. Connors, G. Cartei (Eds.), *Triazenes. Chemical, Biological, and Clinical Aspects*, Plenum Press, New York, **1990**.
[10] D. E. V. Wilman, *Cancer Treat. Rev.* **1988**, *15*, 69–72.
[11] G. F. Kolar in E. Borowski, D. Sugar (Eds.), *Mol. Aspects*

Chemother., Proc. Int. Symp., 2nd, 71–82, Pergamon, New York, **1990**.
[12] A. Gescher, M. D. Threadgill, *Pharmac. Ther.* **1987**, *32*, 191–205.
[13] L. Holleck, G. Kazemifard, *J. Electroanal. Chem.* **1972**, *35*, 369–379.
[14] V. Zvěřina, J. Diviš, J. Marhold, M. Matrka, *Coll. Czech. Chem. Commun.* **1971**, *36*, 1598–1603.
[15] V. Zvěřina, M. Remeš, J. Kroupa, Z. Ságner, M. Matrka, *Coll. Czech. Chem. Commun.* **1972**, *37*, 839–845.
[16] J. Huguet, M. Libert, C. Caullet, *Bull. Soc. Chim. Fr.* **1972**, 4860–4864.
[17] B. Gollas, B. Speiser, *Angew. Chem.* **1992**, *104*, 336–338; *Angew. Chem. Int. Ed. Engl.* **1992**, *31*, 332–334.
[18] B. Speiser, H. Stahl, *Tetrahedron Lett.* **1992**, *33*, 4429–4432.
[19] A. Neudeck, L. Dunsch, *Ber. Bunsenges. Phys. Chem.* **1993**, *97*, 407–411.
[20] T. Suehiro, T. Sato, T. Sano, A. Koike, A. Rieker, *Chem. Lett.* **1989**, 1935–1938.
[21] F. A. Neugebauer, S. Bamberger, W. R. Groh, *Chem. Ber.* **1975**, *108*, 2406–2415.
[22] P. Hertl, A. Rieker, B. Speiser, manuscript in preparation.
[23] S. Bamberger, D. Hellwinkel, F. A. Neugebauer, *Chem. Ber.* **1975**, *108*, 2416–2421.
[24] S. F. Nelsen in *Numerical Data and Functional Relationships in Science and Technology*, vol. II 9/d2, Springer, Berlin, **1980**, p. 22–123.
[25] J.-D. Cheng, H. J. Shine, *J. Org. Chem.* **1975**, *40*, 703–710.
[26] H. G. Viehe, Z. Janousek, R. Merényi, L. Stella, *Acc. Chem. Res.* **1985**, *18*, 148–154.
[27] L. Dunsch, A. Petr, *Ber. Bunsenges. Phys. Chem.* **1993**, *97*, 436–439.
[28] J. Elks, D. H. Hey, *J. Chem. Soc.* **1943**, 441–445.
[29] C. S. Rondestvedt Jr., S. J. Davies, *J. Org. Chem.* **1957**, *22*, 200–203.
[30] L. Hunter, *J. Chem. Soc.* **1937**, 320–324.
[31] A. Wohl, *Bull. Soc. Chim. Fr.* **1938**, 460–468.
[32] B. F. Day, T. W. Campbell, G. M. Coppinger, *J. Am. Chem. Soc.* **1951**, *73*, 4687–4688.
[33] *Organikum*, 15th edition, Deutscher Verlag der Wissenschaften, Berlin, **1984**, p. 655.
[34] K. Scheffler, H. B. Stegmann, *Ber. Bunsenges. Phys. Chem.* **1963**, *67*, 864–867.

[169/94]